Author Manuscript

Author Manuscript

Author Manuscript

Author Manuscript

HHS Public Access

Author manuscript

Mucosal Immunol. Author manuscript; available in PMC 2024 February 05.

Published in final edited form as:

Mucosal Immunol. 2023 December ; 16(6): 843–858. doi:10.1016/j.mucimm.2023.09.004.

Obesity amplifies influenza virus-driven disease severity in male and female mice

Pablo C. Alarcon[1,2,3,4], **Michelle S.M.A. Damen**[1,2], **Cassidy J. Ulanowicz**[1,2,3], **Keisuke Sawada**[1,2,3,4], **Jarren R. Oates**[1,2,6], **Andrea Toth**[1,4,5,6], **Jennifer L. Wayland**[1,2,3,4], **Hak Chung**[1,2], **Traci E. Stankiewicz**[1,2], **Maria E. Moreno-Fernandez**[1,3,7], **Sara Szabo**[1,8], **William J. Zacharias**[1,4,5,6], **Senad Divanovic**[1,2,3,4,9,✉]

[1]Department of Pediatrics, University of Cincinnati College of Medicine, Cincinnati, Ohio, USA.

[2]Division of Immunobiology, Cincinnati Children's Hospital Medical Center, Cincinnati, Ohio, USA.

[3]Immunology Graduate Program, University of Cincinnati College of Medicine, Cincinnati, Ohio, USA.

[4]Medical Scientist Training Program, University of Cincinnati College of Medicine, Cincinnati, Ohio, USA.

[5]Division of Pulmonary Biology, Cincinnati Children's Hospital Medical Center, Cincinnati, Ohio, USA.

[6]Molecular and Developmental Biology Graduate Program, University of Cincinnati College of Medicine, Cincinnati, Ohio, USA.

[7]Division of Gastroenterology, Hepatology and Nutrition Cincinnati Children's Hospital Medical Center, Cincinnati, Ohio, USA.

[8]Division of Pathology, Cincinnati Children's Hospital Medical Center, Cincinnati, Ohio, USA.

[9]Center for Inflammation and Tolerance, Cincinnati Children's Hospital Medical Center, Cincinnati, Ohio, USA.

Abstract

Influenza virus-induced respiratory pneumonia remains a major public health concern. Obesity, metabolic diseases, and female sex are viewed as independent risk factors for worsened influenza virus-induced lung disease severity. However, lack of experimental models of severe obesity in female mice limits discovery-based studies. Here, via utility of thermoneutral housing (30 °C) and

This is an open access article under the CC BY-NC-ND license (http://creativecommons.org/licenses/by-nc-nd/4.0/).

✉ senad.divanovic@cchmc.org .

AUTHOR CONTRIBUTIONS

P.C.A., M.S.M.A.D., and S.D. participated in project conceptualization and study design. W.Z. and A.T. provided virus and aided in study implementation. P.C.A., M.S.M.A.D., C.J.U., K.S., J.R.O., J.L.W., H.C., T.E.S., and M.M.F. participated in data generation and interpretation of data. S.S. provided expertise in histological scoring and provided analysis. P.C.A. and S.D. wrote the manuscript. All authors have contributed to the study and have read and approved the final manuscript.

DECLARATION OF COMPETING INTEREST

The authors have no competing interests to declare.

APPENDIX A. SUPPLEMENTARY DATA

Supplementary data to this article can be found online at https://doi.org/10.1016/j.mucimm.2023.09.004.

Author Manuscript Author Manuscript Author Manuscript Author Manuscript

high-fat diet (HFD) feeding, we induced severe obesity and metabolic disease in female C57BL/6 mice and compared their responses to severely obese male C57BL/6 counterparts during influenza virus infection. We show that lean male and female mice have similar lung edema, inflammation, and immune cell infiltration during influenza virus infection. At standard housing conditions, HFD-fed male, but not female, mice exhibit severe obesity, metabolic disease, and exacerbated influenza disease severity. However, combining thermoneutral housing and HFD feeding in female mice induces severe obesity and metabolic disease, which is sufficient to amplify influenza virus-driven disease severity to a level comparable to severely obese male counterparts. Lastly, increased total body weights of male and female mice at time of infection correlated with worsened influenza virus-driven disease severity metrics. Together, our findings confirm the impact of obesity and metabolic disease as key risk factors to influenza disease severity and present a novel mouse experimental model suitable for future mechanistic interrogation of sex, obesity, and metabolic disease traits in influenza virus-driven disease severity.

BACKGROUND

Influenza virus infection remains a major public health threat. Despite public education and vaccination campaigns, the burden of influenza virus-induced respiratory pneumonia remains high, with an estimated annual 32 million cases and 5.7 million hospitalizations globally[1]. Traditionally, age, chronic pulmonary disease, pregnancy, immunocompromised state, and female sex are viewed as key factors that place individuals at higher risk for worsened influenza disease severity[2]. Additionally, the 2009 H1N1 influenza A pandemic also established obesity as an independent risk factor for influenza disease severity and mortality[3].

Obesity, an unabated pandemic, impacts over half a billion people worldwide[4] and is dogmatically associated with metabolic diseases, including type 2 diabetes, nonalcoholic fatty liver disease (NAFLD), and cardiovascular disease[5]. Individuals with these obesity-associated sequelae have an elevated risk of progressing to severe pneumonia during influenza infection[6,7]. Obesity-associated modulation of the immune system is also linked with enhanced emergence of virulent strains of influenza during infection[8], prolonged viral shedding,[9] and impaired adaptive responses[10] following influenza infection. However, the underlying immunological causes of obesity-associated influenza virus-driven disease severity remain undefined[11].

Sex is another risk factor associated with worsened outcomes during influenza virus infection. Specifically, post-pubertal females exhibit higher morbidity and mortality than their age-matched male counterparts for seasonal and pandemic-related strains of influenza[12,13]. Notably, during the 2009 H1N1 pandemic, females had higher hospitalization and mortality rates than males[14]. In addition, metanalysis of influenza virus challenge studies revealed that females were more likely to develop a higher number of symptoms from the same viral dose when compared to males[15]. However, mechanisms underlying this predisposition to influenza disease severity in females remain underdefined. One underappreciated contributor may be obesity. Pertinently, the global rates of severe obesity are higher in females compared to males[16,17]. Hence, the increased prevalence of severe

Author Manuscript Author Manuscript Author Manuscript Author Manuscript

obesity in females may be linked with the reported increase of influenza virus-driven disease severity. However, despite the clinical significance, epidemiological studies conducted to date have not focused on the intersection of severe obesity, metabolic disease, and sex in influenza disease pathogenesis.

Experimental studies focused on influenza virus-driven disease severity in obesity almost exclusively utilize high-fat diet (HFD)-fed obese male mice. In fact, these severely obese male mice are reported to have higher mortality, lung edema, lung immune cell infiltration, and levels of pro-inflammatory cytokines in their bronchoalveolar lavage fluid (BALF) compared to their lean male counterparts[18]. However, wild-type (WT) C57BL/6 female mice are protected from severe diet-induced obesity (DIO) and metabolic diseases[19]. A potential contributor to the insufficient induction of obesity in C57BL/6 female mice is the ambient housing temperature, which plays a major role in metabolic homeostasis. Animal facilities are predominately maintained at “room temperature” (19 °C–22 °C) for comfort of humans working in these environments. However, the mouse thermoneutral (TN) zone is between 30 °C and 32 °C, and housing below such temperatures exposes mice to chronic thermostress (TS) conditions, which in turn exacerbate stress hormone release (corticosterone and catecholamine), cellular energy expenditure, and immune responses[20].

TN housing at 30 °C supports minimal expenditure of metabolic energy to maintain body temperature[21], alleviating the effects of TS housing and allowing for mice to achieve metabolic homeostasis. Specifically, TN housing, in combination with HFD feeding, increases hepatic inflammation across various models, allowing for female mice to develop NAFLD[22], as well as accentuates the development of atherosclerosis[23], glucose dysmetabolism, and increased visceral adiposity[19]. Thus, the ability of TN housing to promote severe DIO and metabolic diseases in female mice provided a novel and effective model to study influenza virus infection in both obese female and male mice.

In this study, we employed variations in diet (chow diet [CD] *vs.* HFD), housing temperatures (TS *vs.* TN), and sex of mice (male *vs.* female) to determine the contributions of obesity and sex to influenza virus-driven disease severity. To validate successful infections, we used total body weight loss and lung RNA expression of influenza M1 protein, a viral matrix protein present within the cell membrane of infected cells. To analyze influenza disease severity, unflushed left lung weights were used to approximate lung edema and to semiquantitatively examine histopathological changes of lung tissue following influenza virus infection. Further, pro-inflammatory cytokine levels in BALF and lung immune cell (total $CD45^+$ cells, including macrophages and neutrophils) infiltration were used to determine influenza virus-driven lung inflammation and disease severity. Together, we found that lean male and female mice have comparable lung edema, inflammation, and immune cell infiltration during influenza infection. While HFD feeding of male mice in TS conditions is sufficient to induce obesity, metabolic diseases (e.g. visceral adiposity, glucose dysmetabolism, and hepatocellular damage), and worsened influenza virus-driven disease severity, HFD feeding alone at TS is insufficient to induce either severe obesity or amplify influenza virus-driven disease severity in female mice. However, utilizing our novel model of combined TN housing and HFD feeding, we enable the induction of severe obesity and metabolic disease in female mice that fully uncovers phenotypes linked with

Author Manuscript Author Manuscript Author Manuscript Author Manuscript

obesity-associated influenza virus-driven disease severity that is comparable to severely obese male mice. Lastly, we show that increased body weight positively and significantly correlates with worsened influenza virus-driven disease outcomes in both male and female severely obese mice. Collectively, these findings demonstrate the contribution of metabolic disease to influenza virus-driven disease severity in both sexes and highlight the necessity of the future use of robust experimental models of DIO to further interrogate key cellular and molecular mechanisms underlying obesity, metabolic disease, and sex differences in influenza disease pathogenesis.

RESULTS

Lean male and female mice have comparable influenza virus-driven disease severity

To begin to examine the contribution of sex as a variable in influenza virus-driven disease severity, lean, age-matched, male and female mice were intranasally mock infected (saline) or infected with influenza virus (H1N1 PR8; 30HA Units/5.7 $\log_{10}$ 50% Tissue Culture Infectious Dose [$TCID_{50}$]) (Fig. 1A[24,25]). Influenza virus infection induced significant total body weight loss in both male and female mice compared to mock-infected counterparts, although lean female mice displayed reduced weight loss compared to lean male mice (Fig. 1B[24,25]). Further, influenza virus-infected, lean, male and female mice exhibited similar levels of viral M protein transcript expression in the lungs (Fig. 1C[24,25]) and lung edema (weight of non-flushed left lungs) (Fig. 1D[24,25]).

Inflammation and immune cell tissue accrual and function play a central role in influenza virus infection pathogenesis. Lung-produced interleukin-6 (IL-6) is a potential clinical biomarker for worsened influenza virus-driven disease severity[26]. Influenza virus infection similarly increased IL-6 levels in the BALF between lean male and female mice (Fig. 1E[24,25]). Population percentage analyses of lung immune cell populations revealed differences between mock-infected (saline) and influenza virus-infected, lean, male and female mice (Fig. 1F[24,25]). Notably, there were increases in macrophage and neutrophil frequency, lung immune cells known to play roles in influenza virus-driven disease pathogenesis[27,28], and a decrease across all other immune cell populations in influenza-infected mice of both sexes (Fig. 1G[24,25]). Further, lungs from influenza virus-infected, lean mice, compared to mock-infected lean controls, had an overall increase in numbers of $CD45^+$ cells, which was comparable between male and female mice (Fig. 1H[24,25]). Lastly, there were similar increases in macrophage and neutrophil quantified numbers between influenza-infected male and female mice (Figs. 1I and 1J[24,25]). Combined, these data demonstrate that influenza infection utilized in our study robustly drives disease pathogenesis and promotes comparable character and vigor of lung inflammation in lean, age-matched, male and female mice.

HFD feeding exacerbates influenza virus-driven disease severity in male mice

Obesity is an independent risk factor for worsened influenza virus-driven disease outcomes[6,7]. To examine how obesity and metabolic disease shape influenza virus-driven disease severity, male mice were fed CD or HFD and subsequently intranasally mock infected (saline) or infected with influenza virus (Fig. 2A). Obese male mice had

Author Manuscript Author Manuscript Author Manuscript Author Manuscript

significantly decreased time-to-death compared to lean controls within 6 days post-infection (DPI) (Fig. 2B). Temporal analysis of influenza virus-driven disease severity at 1, 3, and 5 DPI revealed that both lean and obese mice infected with influenza virus, compared to mock-infected controls, had significant weight loss that was similar in amplitude (Fig. 2C). Further, infected lean and obese mice had similar expression of viral M protein in their lungs throughout the course of infection (Fig. 2D). However, despite such similarities, lung edema was significantly worsened in influenza virus-infected, obese, male mice, compared to lean, influenza virus-infected controls, at 5 DPI (Fig. 2E).

Obesity skews tissue inflammatory immune responses. Hence, lung immune cell character and inflammatory vigor were examined next. While influenza virus infection resulted in a comparable increase in BALF IL-6 levels at 3 DPI in both lean and obese male mice, the IL-6 levels were significantly higher in obese, compared to lean, male mice at 5 DPI (Fig. 2F). The obese male mice, compared to lean male controls, also had increased total lung $CD45^+$ immune cell accrual at baseline (Fig. 2G, dashed lines). Following influenza virus infection, total lung immune cell accrual was comparable at 3 DPI due to a decrease in obese lung immune cell infiltration but was significantly amplified at 5 DPI in obese mice (Fig. 2G). Notably, at 5 DPI, macrophage and neutrophil numbers were dominantly increased in the lungs of influenza virus-infected, obese, male mice (Figs. 2H and 2I). Additionally, at 5 DPI, IL-6 production by lung $CD45^+$ cells was significantly increased in influenza virus-infected, obese, male mice compared to infected lean male controls (Fig. 2J), with similar trends observed in IL-6 production by lung macrophage populations (Fig. 2K).

We next determined how obesity modifies influenza virus infection-driven tissue pathogenesis. Specifically, left lungs from obese and lean, male, influenza virus-infected and mock-infected mice were histologically examined (Fig. 3A, representative sections at different magnifications). Assessing all histological compartments of the lung, we semi-quantitatively scored inflammatory pathology and expressed these parameters (see materials and methods for specifics) as a combined score of severity of bronchopneumonia for the different experimental conditions. We found that influenza virus-infected, lean and obese, male mice had greater total lung histopathologic severity scores when compared to mock-infected controls. However, the amplitude of the bronchopneumonia severity was similar between influenza virus-infected, lean and obese, male mice (Fig. 3B). Specifically, the bronchocentric histopathologic patterns and the extent of pathologic changes were similar between infected lean and obese male mice (Fig. 3C). Notably, the influenza virus-infected, obese, male mice had a trend toward increased parenchymal inflammation severity scores (peripherally extended and more severe disease) when compared to lean infected controls (Fig. 3D). Combined, our inflammatory and histological findings validate our experimental model by demonstrating that HFD-induced obesity in male mice amplifies influenza virus-driven inflammatory responses in the lung.

HFD feeding alone does not exacerbate influenza virus-driven disease severity in female mice

We next determined whether HFD feeding, independent of severe obesity, is sufficient to similarly exacerbate influenza virus-driven disease severity in female mice. Male and female

Author Manuscript Author Manuscript Author Manuscript Author Manuscript

mice were fed CD or HFD and subsequently infected with influenza virus (Fig. 4A). Of note, female mice fed HFD do not robustly gain weight to be considered “obese” despite being on the “obesogenic diet” for the same length of time as their male counterparts and are thus considered “overweight”. While there was similar weight loss between CD and HFD infected groups of each sex, female mice had less pronounced reduction in absolute weight loss when compared to male mice regardless of diet (Fig. 4B). The expression of influenza virus M protein in the lungs of infected male and female mice, however, was comparable across all conditions (Fig. 4C). Further, lung edema was increased similarly in both HFD-fed, influenza virus-infected, male and female mice compared to their CD-fed counterparts (Fig. 4D). However, while the HFD-fed, influenza virus-infected, female mice tended to have a slightly higher BALF IL-6 levels compared to CD-fed, influenza virus-infected, female mice ($p = 0.07$), such increase was significantly lower compared to HFD-fed, influenza virus-infected, male mice (Fig. 4E). Lastly, HFD-fed, influenza virus-infected, female mice had similar numbers of lung $CD45^+$ cells, macrophages, and neutrophils compared to CD-fed, influenza virus-infected, female mice, but significantly reduced compared to HFD-fed, male mice (Figs. 4F–H). Intriguingly, however, lung immune cell population percentage analysis revealed similar shifts between the HFD-fed, influenza virus-infected, male and female mice (Fig. 4J) when compared to CD-fed, influenza virus-infected, male and female mice (Fig. 4I). Combined, these data suggest that HFD feeding alone is not sufficient to exacerbate inflammatory responses to influenza virus infection in female mice. This is likely due to limited induction of obesity (and absence of severe obesity and metabolic disease) in HFD-fed WT female mice under standard housing (TS) conditions. Further, these data potentially invoke the critical role of severe obesity and metabolic disease in regulation of immune responses to influenza virus infection.

Obesity-associated influenza virus-driven disease severity is maintained in thermoneutrally housed male mice

Housing mice in their TN zone has emerged as a more accurate method of modeling human diseases. Given that TN housing can impact the immune system[29] and inflammatory responses to infection[30,31], we next examined the impact of TN housing on influenza virus-driven disease severity. Lean male mice were placed at TS (22 °C) or TN (30 °C) housing for 4 weeks to acclimate and subsequently infecting with influenza virus (Supplementary Fig. 1A). Influenza virus infection exacerbated body weight loss, viral M protein expression in the lungs, lung edema, and BALF IL-6 levels when compared to saline controls, but to a comparable degree between influenza virus-infected, TS- and TN-housed, lean, male mice (Supplementary Figs. 1B–E). Furthermore, while total lung immune cell infiltration was increased in influenza virus-infected, lean, male mice over mock-infected controls, such increase was similar between TS- and TN-housed infected lean male mice (Supplementary Fig. 1F), a trend also seen in lung macrophage and neutrophil populations (Supplementary Figs. 1G and 1H). Combined, these data suggest that TN housing alone does not alter influenza disease severity in lean male mice.

TN housing also shapes obesity-associated metabolic diseases. Hence, we next examined if TN housing would modify metabolic disease severity in male mice. Age-matched male mice were placed in either TS or TN housing and fed CD or HFD (Supplementary Fig. 2A). TN

Author Manuscript Author Manuscript Author Manuscript Author Manuscript

housing accelerated weight gain in HFD-fed male mice compared to TS-housed HFD-fed males (Supplementary Fig. 2B). However, TN housing did not further exacerbate HFD-induced glucose dysmetabolism (Supplementary Fig. 2C) or epididymal white adipose tissue expansion (Supplementary Fig. 2D). Intriguingly, TN-housed obese males had increased accumulation of perirenal white adipose tissue (Supplementary Fig. 2E) and inguinal white adipose tissue (Supplementary Fig. 2F) compared to TS-housed obese counterparts. Liver weights and hepatocellular damage (measured via serum alanine transaminase [ALT] levels) in HFD-fed males were also further increased by TN housing (Supplementary Figs. 2G and 2H). Combined, these data suggest that TN housing exacerbates severity of specific metabolic disease parameters in obese male mice.

The contribution of TN-housing amplification of metabolic disease parameters to influenza virus-driven disease severity in obese male mice was examined next. HFD-fed obese male mice were housed in TS or TN conditions and were either intranasally mock-infected or infected with influenza virus (Fig. 5A). Although HFD-fed, TN-housed, mock-infected male mice exhibited weight loss post-challenge, the HFD-fed, influenza virus-infected, male mice had a greater amplitude of the weight loss in both TS and TN conditions (Fig. 5B). Similarly, lung viral M protein expression, left lung weight, and BALF IL-6 levels were significantly elevated over mock-infected controls but were found comparable between the obese, influenza virus-infected, male mice housed at TS and TN (Figs. 5C–E). Further, obese male mice infected with influenza virus had increased numbers of $CD45^+$ cells, macrophages, and neutrophils in the lungs compared to mock-infected controls, albeit such increase was similar between TS- and TN-housed mice (Figs. 5F–H). Finally, lung immune cell population analysis revealed a high degree of similarity in lung population percentages in mock-infected mice in TS or TN housing (Fig. 5I). During influenza virus infection, however, TN-housed mice had a slight increase in lung macrophage percentage infiltration when compared to TS-housed mice (Fig. 5J). Combined, these data suggest that HFD feeding in TN housing does not robustly modify influenza virus-driven disease severity in either the lean or obese male mice.

TN housing establishes DIO-associated influenza virus-driven disease severity in female mice

TN housing in combination with HFD feeding can amplify metabolic disease outcomes in male mice.[19] Hence, we next re-examined such outcomes in female mice. Age-matched female mice were housed under TS or TN conditions and fed CD or HFD (Supplementary Fig. 3A). TN-housed female mice fed HFD gained significantly more weight when compared to TS-housed HFD-fed counterparts or either TS- or TN-housed CD-fed controls (Supplementary Fig. 3B). Further, such increase in obesity positively correlated with increased accumulation of gonadal white adipose tissue (Supplementary Fig. 3C), perirenal white adipose tissue (Supplementary Fig. 3D), and inguinal white adipose tissue (Supplementary Fig. 3E) when compared to TS-housed HFD-fed females and TN-housed CD-fed controls. Notably, only TN-housed HFD-fed female mice developed glucose dysmetabolism (Supplementary Fig. 3F) and had increased liver weights and serum ALT levels (Supplementary Figs. 3G and 3H). Combined, these data confirmed that TN housing

Author Manuscript Author Manuscript Author Manuscript Author Manuscript

also allows for development of HFD-induced obesity and metabolic diseases in WT female mice.

Whether TN housing impacts influenza virus-driven disease severity in lean female mice was examined next. Female mice were fed CD and housed at TS or TN conditions for 4 weeks to acclimate prior to influenza virus infection (Supplementary Fig. 4A). Housing conditions did not modify influenza virus infection-driven total body weight loss (Supplementary Fig. 4B). However, TN-housed lean females had increased lung edema (Supplementary Fig. 4D). Lung viral M protein transcript expression (Supplementary Fig. 4C) and BALF IL-6 levels (Supplementary Fig. 4E), while elevated over mock-infected controls, were comparable between influenza virus-infected, TS- and TN-housed females. Lastly, total lung immune cell infiltration (Supplementary Fig. 4F), as well as lung macrophages and neutrophils numbers (Supplementary Figs. 4G and 4H), were similar between influenza virus-infected, TN- and TS-housed, female mice. Combined, these data suggest that TN housing has minimal impact on influenza virus-driven disease severity in lean female mice.

To examine the impact of severe obesity and metabolic diseases on influenza virus-driven disease severity in female mice, mice were housed at TS or TN conditions and fed HFD prior to influenza virus infection (Supplementary Fig. 5A). TN-housed, influenza virus-infected, female mice had increased total body weight loss compared to their TS-housed controls (Supplementary Fig. 5B). Lung viral M protein transcript expression, lung edema, and BALF IL-6 levels were similarly elevated in influenza virus-infected, TS and TN, HFD-fed, housed mice (Supplementary Figs. 5C–E). However, influenza virus infection induced increased numbers of lung $CD45^+$ cells, macrophages, and neutrophils in the TN-housed obese female mice when compared to the TS-housed HFD-fed female control mice (Supplementary Figs. 5F–H). Combined, these data suggest that a combination of HFD feeding and TN housing establishes robust obesity-associated influenza disease severity in female mice.

Obese male and female mice with metabolic disease have comparable influenza virus-driven disease severity

Whether the independent risk factors of obesity-associated metabolic disease and sex (female) have a synergistic impact on worsened influenza virus-driven infection disease outcomes remains unknown. To examine such possibilities, TN-housed male and female mice were placed on CD or HFD and infected with influenza virus (Fig. 6A). All infected mice, regardless of sex and diet, had comparable total body weight loss (Fig. 6B) and lung viral M protein expression (Fig. 6C). Obese, influenza virus-infected, female mice had significantly worse lung edema and elevated BALF IL-6 levels when compared to lean female controls, which was exacerbated to a similar degree to obese, influenza virus-infected, male mice (Figs. 6D and 6E). Further, both obese male and female mice had robust increase in total lung immune cell accrual compared to their lean counterparts (Fig. 6F), in contrast to TS-housed HFD-fed influenza-infected female mice (Fig. 4F). Additionally, lung macrophage and neutrophil populations were also increased obese male and female mice when compared to lean counterparts (Figs. 6G and 6H). These trends were also visible

Author Manuscript Author Manuscript Author Manuscript Author Manuscript

in the population percentage analysis when lean, influenza virus-infected, male and female mice (Fig. 6I) were compared to the obese influenza virus-infected counterparts (Fig. 6J). Semiquantitative analyses of histopathologic images (Fig. 6K) revealed that bronchocentric and parenchymal pathologic patterns were comparable across all infected conditions, regardless of sex or diet (Figs. 6L and 6M). Notably, variable correlation analyses were performed between body weight and disease severity metrics. These tests showed significant positive correlation between heavier body weight preinfection and increased lung edema (Fig. 7A), BALF IL-6 levels (Fig. 7B), and total immune cell accrual (Fig. 7C) at 5 DPI in TN-housed male and female mice.

Lastly, all examined metrics of disease severity (weight loss, left lung weight, lung viral M protein transcript expression, BALF IL-6 levels, and lung immune cell infiltration) are summarized for CD- versus HFD-fed and male versus female mice under TS conditions in Table 1 and TN conditions in Table 2. Combined, our data suggest that TN housing is a novel and viable method of inducing severe obesity in female mice, which upon influenza virus infection develop robust obesity-associated influenza disease severity to a comparable degree as their severely obese male counterparts.

DISCUSSION

In this study, we aimed to verify the impact of obesity and obesity-associated metabolic diseases as key risk factors to influenza disease severity and to establish a novel mouse model of severe obesity in female mice that can be utilized for future mechanistic interrogations on the role of sex and metabolic disease in shaping influenza virus-driven disease severity in obesity. We found that HFD-driven obesity accelerated time-to-death due to influenza virus infection in male mice. However, HFD feeding alone was not sufficient to induce obesity-associated influenza virus-driven disease severity in female mice housed under traditional (TS) conditions. Importantly, combination of HFD feeding and TN housing was required to promote severe obesity and metabolic disease in female mice and enable initial characterization of influenza virus-driven disease severity in this setting. Combined, our findings demonstrate that TN-housed, severely obese, male and female mice had similarly exacerbated inflammatory responses to high-dose influenza virus challenge and that mouse body weight preinfection strongly correlated with influenza disease severity outcomes.

Unlike previous reports[32], our initial findings suggested that lean male and female mice have similar influenza virus-driven disease severity. A potential explanation for the divergent outcomes may be the difference in the dose of influenza virus employed. While some influenza infection models suggest that lean female mice exhibit greater reductions in body mass, body temperature, and survival while having increased BALF pro-inflammatory cytokines (e.g. IL-6, tumor necrosis factor, and interferon [IFN]-γ) levels in spite of similar viral titers[33], other studies suggest that these responses are dose-dependent and not present in models employing higher viral dosage and severe influenza infection[32]. Thus, a high dose of influenza virus used in our studies may represent a severe influenza virus-driven disease that masks sex differences previously reported at lower doses. Hence, future studies utilizing a gradient of viral titers (e.g. low, medium, and high) in tandem with our novel model

Author Manuscript Author Manuscript Author Manuscript Author Manuscript

may be needed to fully uncover sex-specific phenotypes of obesity-associated influenza virus-driven disease pathogenesis.

Historically, WT C57/BL6 female mice are protected from DIO and obesity-associated metabolic diseases[34]. Our findings suggested that placing female mice on HFD in traditional TS housing results in a minor weight gain (overweight) and minimally exacerbated inflammation during influenza infection when compared to HFD-fed, severely obese male mice housed at TS. Alternative models of obesity in female mice utilize genetic manipulation of the leptin hormone to generate obesity (*ob/ob* mice)[35]. While successful in generating female mice with metabolic disease, elimination of this key endocrine hormone may introduce confounding variables in the context of influenza virus infection. Specifically, leptin plays an inflammatory role in the immune system, including its effects on cells necessary for proper responses to influenza virus infection (e.g. macrophages, neutrophils, natural killer cells)[36]. Further, leptin has been appreciated to play an important role in lung development and homoestasis[37,38], thus questioning the applicability of leptin-deficient mice in the context of lung-tropic infections.

The temperature for traditional housing (22 °C) is chosen for human comfort in animal facilities. Thus, mice kept in traditional housing experience chronic cold stress, which impacts their metabolic health. While in this temperature WT male mice are still able to develop DIO, WT females are resistant to severe obesity, limiting the range of studies that can be performed. In fact, housing mice in their TN zone (30 °C–32 °C) achieves a metabolic homeostasis. TN housing has been shown to reduce heart rate by over 200 beats per minute, decrease mean arterial blood pressure by 30%, and decrease energy expenditure by 50%–60% in mice[29,39]. Furthermore, TN housing improves the murine model of DIO in male mice by exacerbating adipose tissue inflammation[23], allowing for the development of atherosclerotic plaques[40], and improving the NAFLD pathogenesis model[22]. Additionally, our previous findings suggest that utilizing TN housing allows for WT female mice to also develop DIO and metabolic disease[19]. Hence, these data provided a platform to begin to establish a novel methodology to examine whether severe obesity shapes influenza virus-driven disease severity in female mice.

Whether TN housing independently alters the immune response to influenza virus infection is insufficiently defined. Existing literature suggests that housing temperature plays an important role in inflammatory immune responses. For example, TN housing is reported to increase systemic inflammation, elevate levels of circulating pro-inflammatory cytokines[40], and promote febrile responses to LPS challenge[30]. This increased inflammatory phenotype is also noted in the context of infection, with a more robust immune response to rhinovirus[41] and *E. coli*[42]. However, contrary results in infection have also been reported. Specifically, TN housing is shown to decrease mortality to Typhus[43] and rabies[44]. In context of respiratory disease-associated pathologies, TN housing is shown to increase T_{reg} cell lung infiltration in murine asthma models[45] and decrease inflammatory cytokine responses to influenza virus infection in the lung 72 hours post-infection[46]. Thus, these findings made it imperative to determine whether TN housing impacted obesity-associated influenza virus-driven disease severity in male mice where an established phenotype in TS housing already exists. Notably, our data demonstrate that obesity-associated influenza virus-driven disease

Author Manuscript Author Manuscript Author Manuscript Author Manuscript

severity is similar in TN- and TS-housed, lean mice and is comparably induced in TN- and TS-housed, obese male mice.

In our studies, we observed that TN-housed obese, mock-infected, male mice had notable weight loss when compared to the mock-infected TS-housed obese controls. A possible explanation for this effect could be associated with the setup of our studies. Specifically, after male mice become obese in either TN or TS housing, all mice are moved to an animal facility uniquely used for infectious studies that is maintained at TS housing conditions until conclusion of the study. As such, due to the change in ambient temperatures the weight loss experienced by the TN-housed may be augmented. However, the total weight loss by the mock-infected, TN-housed, obese male mice was not as extensive as that observed in the TN-housed, influenza virus-infected mice. Importantly, the examined metrics of influenza virus-driven disease severity were comparable among influenza virus-infected, TS- and TN-housed, severely obese, male mice. These data suggest that the potential difference in weight loss in TN-housed, obese male mice is an unlikely contributor to their exacerbated lung inflammatory state following influenza virus infection.

Although studies have shown that females in their reproductive years are at a higher risk of developing worsened disease outcomes to influenza virus infection[14,15], epidemiological studies to date have not examined whether this predisposition is due to the higher global rates of female obesity[17]. While pregnancy is an independent risk factor for influenza virus-driven disease severity[47,48], published reports have suggested that pregnancy by itself does not fully account for the increased female predisposition to influenza disease severity[13,49]. Thus, increased global obesity rates in females may contribute to the skewed female morbidity and mortality rates with regards to influenza virus infection. Therefore, additional epidemiological studies are warranted to fully elucidate both the individual and combined contribution of obesity and sex to influenza virus-driven disease severity.

While rigorously performed, there are still several limitations to our studies. One key limitation is the usage of a lethal viral dose. While most influenza infection survival studies extend past 2 weeks, our studies are limited to day 5 post-infection as obese mice had substantial mortality beginning at day 6 (Fig. 2B). Further, lean mice, regardless of their housing or sex, had the maximum percent weight loss allowed by animal care standards at 5 DPI (data not shown). Given these limitations, key future directions include additional studies at a range of viral doses (e.g. low, medium, high) followed by temporal analysis of disease severity phenotypes in obese state in both sexes. Another limitation is the lack of mechanistic exploration underlying obesity-associated exacerbation of influenza virus-driven disease severity. Although our study does not address the mechanisms underlying increased disease severity in obesity, importantly, it presents the newly established model of combined TN housing and HFD feeding that provides a robust platform to conduct these future mechanistic studies. In particular, the positive and significant correlation between increased body weight and influenza disease severity (Fig. 6) reveals the need for further studies that interrogate the causative molecular and cellular causes of this phenotype. While our studies did not reveal major differences in immune cell accrual and inflammatory capacity between obese male and female mice infected with high doses of influenza virus, this may be due to the state of the immune system during obesity or the dose of influenza

Author Manuscript Author Manuscript Author Manuscript Author Manuscript

virus used. Obesity represents a chronic inflammatory state[50], and thus such skewing may exacerbate or tolerize the inflammatory response in obese males and females to a degree where they equilibrate, resulting in similar influenza virus-driven disease severity.

TN housing represents an important tool to mechanistically interrogate how obesity-induced metabolic changes alter key immune mediators. Various mechanisms are likely at play, including pro-inflammatory cytokines, adipokines, and hormones. For example, Type I IFNs, key modulators of immune responses, play a critical role in influenza virus infection. Type I IFN responses are reported to be more robust in females than males[51], and type I IFN levels are also elevated during the obese state[52]. Hence, how modulation of type I IFN axis shapes influenza virus-driven disease severity in obesity and sex is a prime candidate for future studies. Another potential mechanism is the leptin signaling pathway. Leptin levels are increased in obesity[53] and differ between males and females[54]. Further, given leptin's proinflammatory effect on immune cells[36], future examination of the mechanistic role of leptin to obesity-associated inflammatory responses in influenza virus-driven disease severity in obesity and sex would be imperative. The role of sex-specific hormones should also be interrogated. Of note, estrogen has an anti-inflammatory effect on immune cells,[55] and estrogen levels are elevated in obesity[56]. Thus, future analysis of the role of estrogen in influenza virus-driven disease severity in obesity and sex is needed.

Other applications of our model include future studies utilizing non-lethal doses to examine processes underlying lung tissue repair between obese male and female mice. As lung repair is impaired in obese male mice[57], such studies would be highly informative. Further, obese male mice have diminished adaptive immune responses to influenza virus infection[10]. Our model can also be utilized to uncover the existence of potential sex-specific differences in the adaptive immune responses to influenza virus via re-infection challenge experiments in obese hosts. Lastly, sex-dependent differences are reported for multiple infectious diseases[58], including tuberculosis[59] and severe acute respiratory syndrome-coronavirus 2[60,61]. Thus, our novel model represents an ideal platform from which to examine the role of sex and metabolic disease in the pathogenesis of various infections. Collectively, utilizing the combined HFD-feeding and TN-housing model allows for rigorous and comparative interrogation of molecular and cellular modifiers of inflammatory immune responses across numerous insults in obese male and female mice. The discovery of novel mechanistic insights, via the utility of these platforms, may allow for development of more targeted therapies in the obese population to combat infectious diseases, with their sex as a careful consideration for disease severity outcomes.

MATERIALS AND METHODS

All animal care was provided in accordance with the Guide for the Care and Use of Laboratory Animals. All studies were approved by the Cincinnati Children's Hospital Medical Center (CCHMC) Institutional Animal Care and Use Committee.

Mouse obesogenic diet model

WT mouse breeding pairs, originally purchased from Jackson Laboratories (Bar Harbor, ME, USA), were on C57BL/6J background, housed at TS (22 °C) conditions with free

Author Manuscript Author Manuscript Author Manuscript Author Manuscript

access to autoclaved food and water, and bred at CCHMC in a specific pathogen-free facility with free access to autoclaved CD food (LAB Diet #5010; calories provided by carbohydrates [58%], fat [13%], and protein [29%]) and water. 6- to 8-week-old, WT, male and female mice were used in our studies. For all studies, food and water were replaced weekly. For obesogenic model studies, age-matched mice were fed either CD or an irradiated HFD Research Diets #D12492i; 60% of calories from fat). Body weight was recorded weekly. Corn cob bedding was used in the housing of all mice.

For TN studies, 6- to 8-week-old mice were maintained at TS or placed at TN (30 °C with 30% humidity) conditions for 2 weeks to allow acclimation prior to the initiation of dietary challenge. TN housing was accomplished using Caron chambers (Caron Products & Services, Inc, Marietta, OH, USA). Age-matched mice were fed CD or HFD, with food and water replaced weekly. Body weights were recorded weekly.

For glucose tolerance tests, fasted mice were subjected to glucose (mice injected 100 μL of a 10% dextrose solution per gram of body weight), and glucose was monitored kinetically using an Accu-Chek glucometer per manufacturer instructions and as done previously by our laboratory[19,22]. For hepatocellular damage assessment, serum ALT levels were quantified using ALT Reagent and Catatrol I and II (Catachem, Oxford, CT, USA).

$TCID_{50}$

To determine viral dosage, a $TCID_{50}$ assay utilizing Madin-Darby Canine Kidney cells in monolayer was performed as described previously[62]. In brief, Madin-Darby Canine Kidney monolayers in 96-well tissue culture-treated plates were infected with serially diluted (10-fold) viral stock (starting at 30 HA Units). Plates were incubated at 37 °C for 7 days before being fixed (4% paraformaldehyde) for 1–3 hours and subsequently stained (Naphthol Blue-Black dye) overnight. Plates were subsequently washed and examined under light microscope for cytopathic effect. A positive signal was interpreted as well where cells had more than 50% cytopathic effect. $TCID_{50}$ was calculated using the Reed-Muench method.

In vivo influenza Infections

Mice were moved from their TS or TN housing to a dedicated infectious room in the CCHMC animal facility (infectious room kept at standard temperature of 22 °C). Mice were sedated via isoflurane inhalation (2.5% isoflurane; Akorn, NDC 59399-106-01) and treated intranasally with saline (50 μL, veterinary grade; Hospira, NDC 0409-4888-02) or H1N1 PR8 influenza (30 HA Units/7.16 $\log_{10}$EID/5.7 $\log_{10}TCID_{50}$ in 50 μL veterinary grade saline; Charles River: Influenza A/PR/8/34, Batch: 4XP160913; provided by Dr William Zacharias). Mice were subsequently monitored (weight measured daily) before tissue collection at 1, 3, or 5 DPI.

Quantitative real-time reverse transcriptase polymerase chain reaction

Lung tissue samples were homogenized in TRIzol (Invitrogen, Waltham, MA, USA), followed by messenger RNA extraction and reverse transcription to cDNA (Verso cDNA Synthesis Kit; Thermo Scientific, Waltham, MA, USA). Quantitative polymerase chain reaction was done utilizing QuantStudio 7 Real-Time polymerase chain reaction System

Author Manuscript Author Manuscript Author Manuscript Author Manuscript

(Applied Biosystems, Waltham, MA, USA) according to the manufacturer's instructions. Primer sequences used for the influenza M1 protein gene were as follows:

Influenza M1 protein Sense: 5′-AAG ACC AAT CCT GTC ACC TCT GA-3′

Influenza M1 protein Antisense: 5′-CAA AGC GTC TAC GCT GCA GTC C-3′

BALF cytokine quantification

BALF was obtained post-exsanguination of mouse. A cross-section incision was made on the exposed trachea. Following, a cannula was inserted, and the lung was flushed 3–4 times with 1 mL of Hanks' Balanced Salt Solution (Gibco, Billings, MT, USA). Recovered fluid was placed into a 1.5 mL Eppendorf tube. BALF was subsequently centrifugated at 300*g* for 6 minutes and then at 5000*g* for 30 seconds. Fluid was separated from the pelleted lung cells. BALF IL-6 was quantified by enzyme-linked immunosorbent assay (BD Biosciences, Franklin, Lakes, NJ.) as per manufacturer instructions.

Lung immune cell isolation and flow cytometric analysis

To determine immune cell populations, lungs were digested (digestion buffer: 7 mL/sample Dulbecco's modified Eagle's medium + 4-(2-hydroxyethyl)-1-piperazineethanesulfonic acid, 2% bovine serum albumin, 0.03 mg/mL Liberase Blendzyme 3 Collagenase Cocktail, 50 U/mL DNAse) and immune cells were isolated. Cells were stimulated for 4 hours with phorbol 12-myristate 13-acetate (50 ng/mL; Sigma-Aldrich), Ionomycin (1 μg/mL; Calbiochem), and brefeldin A. Cells were subsequently labeled with monoclonal antibodies. Specifically, Live/dead (Zombie UV Dye; BioLegend, San Diego, CA, USA), B220 – BV605 (clone RA3–6B2, BioLegend), CD45 – PEDazzle (clone 104, BioLegend), CD11b – eFluor450 (clone M1/70, eBioscience, San Diego, CA, USA), CD11c – BV711 (clone N418, BioLegend), NK1.1 – FITC (clone PK136, BioLegend), F4/80 – AF700 (clone BM8, eBioscience), Gr1 – APC (clone RB6–8C5, eBioscience), CD8 – BV510 (clone 53–6.7, BioLegend), and IL6 – PE (clone MP5–20F3, eBioscience). Data were collected using an LRS Fortessa flow cytometer (BD Biosciences) and analyzed by FlowJo X software (vX10, Tree Star, Ashland, OR, USA).

Histopathological analysis

For all mice, left lungs were identically clamped with a hemostat during BALF isolation before being removed from chest cavity (no infusion, flushing, or inflation performed). For histology, left lung tissue was fixed in 10% buffered formalin and stained with hematoxylin & eosin. Evaluation was performed by an experienced board-certified pathologist who was blinded to the experimental parameters while scoring. Semiquantitative assessment determined: (1) inflammatory severity/grade of bronchopneumonia (none, mild, moderate, severe); (2) inflammatory activity and composition (from neutrophil-predominant, purulent necrotizing, to lymphomononuclear-predominant, with histiocytes and plasma cells); (3) "bronchitis" to "bronchiolitis" to "pneumonia" at major histologic landmarks of the conductive airways to airspaces, from the proximal segmental bronchial level, (through bronchioles, terminal and respiratory bronchioles) to alveolar ducts, sacs, and alveoli; and (4) alveolar involvement and compromise, (here referred to as "parenchymal inflammation")

Author Manuscript Author Manuscript Author Manuscript Author Manuscript

secondary both to (a) extension of inflammation along the conductive airways/bronchial tree to air spaces/alveoli in the peripheral lung, and (b) centrally, via direct peribronchial extension of marked purulent bronchitis (from the lumen through the wall). Parameters were quantified in a total combined score for the purposes of semiquantitative comparison of influenza disease severity; predominantly intraluminal airway-disease (bronchocentric) versus additional significant involvement of alveolated parenchyma (parenchymal) were also accounted for in scoring.

Statistical analysis

For statistical analysis, normality and lognormality tests and parametric tests were employed as necessary via the Prism 5a software (GraphPad Software Inc, San Diego, CA, USA). For all normally distributed data sets, unpaired two-tailed Student's t test was used when the comparison was between 2 groups, and a one-way analysis of variance with Tukey's post hoc test to assess differences between specific groups was employed for 3 or more groups. For variable correlation analyses, nonparametric Spearman Rank Correlation tests were performed on datasets with smaller power, and Pearson Correlation tests were performed on datasets with a larger *n*. Statistical analysis was completed using Prism 5a. All values are represented as means ± standard error of the mean. A p-value < 0.05 was considered significant. Sample size determination was based on preliminary data with respect to influenza infection including weight loss, lung immune cell infiltration, and lung viral M protein expression. No animals were excluded from analyses.

Supplementary Material

Refer to Web version on PubMed Central for supplementary material.

ACKNOWLEDGMENTS

The work for this manuscript was supported in part by the National Institutes of Health R01DK099222 (to S.D.) CCHMC Research Innovation and Pilot funding (to S.D.), and National Institutes of Health 1F31AI169757-01 (to P.C.A.). Variable correlation analyses were validated by Dr Todd Jenkins. Images for figures created with BioRender.com.

DATA AVAILABILITY

The datasets generated and analyzed during the current study are available from the corresponding author on reasonable request.

REFERENCES

1. Uyeki TM, Hui DS, Zambon M, Wentworth DE & Monto AS Influenza. Lancet 400, 693–706 (2022). [PubMed: 36030813]
2. Van Kerkhove MD et al. Risk factors for severe outcomes following 2009 influenza A (H1N1) infection: a global pooled analysis. PLoS Med 8:e1001053.
3. Writing Committee of the WHO Consultation on Clinical Aspects of Pandemic (H1N1) 2009 Influenza et al. Clinical aspects of Pandemic 2009 influenza A (H1N1) virus infection. N. Engl. J. Med 362, 1708–1719 (2010). [PubMed: 20445182]

Author Manuscript Author Manuscript Author Manuscript Author Manuscript

4. Finucane MM et al. National, regional, and global trends in body-mass index since 1980: systematic analysis of health examination surveys and epidemiological studies with 960 country-years and 9·1 million participants. Lancet 377, 557–567 (2011). [PubMed: 21295846]
5. Collaboration PS et al. Body-mass index and cause-specific mortality in 900 000 adults: collaborative analyses of 57 prospective studies. Lancet 373, 1083–1096 (2009). [PubMed: 19299006]
6. Allard R, Leclerc P, Tremblay C & Tannenbaum TN Diabetes and the severity of pandemic influenza A (H1N1) infection. Diabetes Care 33, 1491–1493 (2010). [PubMed: 20587722]
7. Papic N et al. Liver involvement during influenza infection: perspective on the 2009 influenza pandemic. Influenza Other Respir. Viruses 6, e2–e5 (2012). [PubMed: 21951624]
8. Honce R et al. Obesity-related microenvironment promotes emergence of virulent influenza virus strains. mBio 11, e03341–e3419 (2020). [PubMed: 32127459]
9. Maier HE et al. Obesity increases the duration of influenza A virus shedding in adults. J. Infect. Dis 218, 1378–1382 (2018). [PubMed: 30085119]
10. Karlsson EA, Sheridan PA & Beck MA Diet-induced obesity impairs the T cell memory response to influenza virus infection. J. Immunol 184, 3127–3133 (2010). [PubMed: 20173021]
11. Alarcon PC et al. Adipocyte inflammation and pathogenesis of viral pneumonias: an overlooked contribution. Mucosal Immunol 14, 1224–1234 (2021). [PubMed: 33958704]
12. Klein SL & Flanagan KL Sex differences in immune responses. Nat. Rev. Immunol 16, 626–638 (2016). [PubMed: 27546235]
13. Campbell A et al. Risk of severe outcomes among patients admitted to hospital with pandemic (H1N1) influenza. CMAJ 182, 349–355 (2010). [PubMed: 20159893]
14. Klein SL, Passaretti C, Anker M, Olukoya P & Pekosz A The impact of sex, gender and pregnancy on 2009 H1N1 disease. Biol. Sex Differ 1, 5 (2010). [PubMed: 21208468]
15. Giurgea LT et al. Sex differences in influenza: the challenge study experience. J. Infect. Dis 225, 715–722 (2022). [PubMed: 34423369]
16. Jacobsen H & Klein SL Sex differences in immunity to viral infections. Front. Immunol 12:720952.
17. Boutari C & Mantzoros CSA 2022 update on the epidemiology of obesity and a call to action: as its twin COVID-19 pandemic appears to be receding, the obesity and dysmetabolism pandemic continues to rage on. Metabolism 133:155217. [PubMed: 35584732]
18. Honce R & Schultz-Cherry S Impact of obesity on influenza A virus pathogenesis, immune response, and evolution. Front. Immunol 10, 1071 (2019). [PubMed: 31134099]
19. Giles DA et al. Thermoneutral housing exacerbates nonalcoholic fatty liver disease in mice and allows for sex-independent disease modeling. Nat. Med 23, 829–838 (2017). [PubMed: 28604704]
20. Bowers SL, Bilbo SD, Dhabhar FS & Nelson RJ Stressor-specific alterations in corticosterone and immune responses in mice. Brain Behav. Immun 22, 105–113 (2008). [PubMed: 17890050]
21. Karp CL Unstressing intemperate models: how cold stress undermines mouse modeling. J. Exp. Med 209, 1069–1074 (2012). [PubMed: 22665703]
22. Oates JR et al. Thermoneutral housing shapes hepatic inflammation and damage in mouse models of non-alcoholic fatty liver disease. Front. Immunol 14:1095132.
23. Tian XY et al. Thermoneutral housing accelerates metabolic inflammation to potentiate atherosclerosis but not insulin resistance. Cell Metab 23, 165–178 (2016). [PubMed: 26549485]
24. Moreno-Fernandez ME et al. PKM2-dependent metabolic skewing of hepatic Th17 cells regulates pathogenesis of non-alcoholic fatty liver disease. Cell Metab 33, 1187–1204.e9 (2021). [PubMed: 34004162]
25. Chan CC et al. Type I interferon sensing unlocks dormant adipocyte inflammatory potential. Nat. Commun 11, 2745 (2020). [PubMed: 32488081]
26. Paquette SG et al. Interleukin-6 is a potential biomarker for severe pandemic H1N1 influenza A infection. PLoS One 7, e38214 (2012). [PubMed: 22679491]
27. Hoeve MA, Nash AA, Jackson D, Randall RE & Dransfield I Influenza virus A infection of human monocyte and macrophage subpopulations reveals increased susceptibility associated with cell differentiation. PLoS One 7, e29443 (2012). [PubMed: 22238612]

Author Manuscript Author Manuscript Author Manuscript Author Manuscript

28. Moorthy AN, Tan KB, Wang S, Narasaraju T & Chow VT Effect of high-fat diet on the formation of pulmonary neutrophil extracellular traps during influenza pneumonia in BALB/c mice. Front. Immunol 7, 289 (2016). [PubMed: 27531997]
29. Stemmer K et al. Thermoneutral housing is a critical factor for immune function and diet-induced obesity in C57BL/6 nude mice. Int. J. Obes. (Lond) 39, 791–797 (2015). [PubMed: 25349057]
30. Rudaya AY, Steiner AA, Robbins JR, Dragic AS & Romanovsky AA Thermoregulatory responses to lipopolysaccharide in the mouse: dependence on the dose and ambient temperature. Am. J. Physiol. Regul. Integr. Comp. Physiol 289, R1244–R1252 (2005). [PubMed: 16081879]
31. Rice P et al. Febrile-range hyperthermia augments neutrophil accumulation and enhances lung injury in experimental gram-negative bacterial pneumonia. J. Immunol 174, 3676–3685 (2005). [PubMed: 15749906]
32. Lorenzo ME et al. Antibody responses and cross protection against lethal influenza A viruses differ between the sexes in C57BL/6 mice. Vaccine 29, 9246–9255 (2011). [PubMed: 21983155]
33. Larcombe AN et al. Sexual dimorphism in lung function responses to acute influenza A infection. Influenza Other Respir. Viruses 5, 334–342 (2011). [PubMed: 21668688]
34. Pettersson US, Waldén TB, Carlsson PO, Jansson L & Phillipson M Female mice are protected against high-fat diet induced metabolic syndrome and increase the regulatory T cell population in adipose tissue. PLoS One 7, e46057 (2012). [PubMed: 23049932]
35. Wang B, Chandrasekera PC & Pippin JJ Leptin- and leptin receptor-deficient rodent models: relevance for human type 2 diabetes. Curr. Diabetes Rev 10, 131–145 (2014). [PubMed: 24809394]
36. Francisco V et al. Obesity, fat mass and immune system: role for leptin. Front. Physiol 9, 640 (2018). [PubMed: 29910742]
37. Huang K et al. Effects of leptin deficiency on postnatal lung development in mice. J. Appl. Physiol 1985(105), 249–259 (2008).
38. Jutant EM, Tu L, Humbert M, Guignabert C & Huertas A The thousand faces of leptin in the lung. Chest 159, 239–248 (2021). [PubMed: 32795478]
39. Maloney SK, Fuller A, Mitchell D, Gordon C & Overton JM Translating animal model research: does it matter that our rodents are cold? Physiology (Bethesda) 29, 413–420 (2014). [PubMed: 25362635]
40. Giles DA et al. Modulation of ambient temperature promotes inflammation and initiates atherosclerosis in wild type C57BL/6 mice. Mol. Metab 5, 1121–1130 (2016). [PubMed: 27818938]
41. Foxman EF et al. Temperature-dependent innate defense against the common cold virus limits viral replication at warm temperature in mouse airway cells. Proc. Natl Acad. Sci. U. S. A 112, 827–832 (2015). [PubMed: 25561542]
42. Liu E et al. Naturally occurring hypothermia is more advantageous than fever in severe forms of lipopolysaccharide- and Escherichia coli-induced systemic inflammation. Am. J. Physiol. Regul. Integr. Comp. Physiol 302, R1372–R1383 (2012). [PubMed: 22513748]
43. Moragues V & Pinkerton H Variation in morbidity and mortality of murine typhus infection in mice with changes in the environmental temperature. J. Exp. Med 79, 41–43 (1944). [PubMed: 19871351]
44. Bell JF & Moore GJ Effects of high ambient temperature on various stages of rabies virus infection in mice. Infect. Immun 10, 510–515 (1974). [PubMed: 4426698]
45. Liao W et al. Thermoneutral housing temperature regulates T-regulatory cell function and inhibits ovabumin-induced asthma development in mice. Sci. Rep 7, 7123 (2017). [PubMed: 28769099]
46. Jhaveri KA, Trammell RA & Toth LA Effect of environmental temperature on sleep, locomotor activity, core body temperature and immune responses of C57BL/6J mice. Brain Behav. Immun 21, 975–987 (2007). [PubMed: 17467232]
47. Jamieson DJ et al. H1N1 2009 influenza virus infection during pregnancy in the USA. Lancet 374, 451–458 (2009). [PubMed: 19643469]
48. Louie JK, Acosta M, Jamieson DJ & Honein MA & California Pandemic (H1N1) Working Group. Severe 2009 H1N1 influenza in pregnant and postpartum women in California. N. Engl. J. Med 362, 27–35 (2010). [PubMed: 20032319]

Author Manuscript Author Manuscript Author Manuscript Author Manuscript

49. Kumar A et al. Critically ill patients with 2009 influenza A(H1N1) infection in Canada. JAMA 302, 1872–1879 (2009). [PubMed: 19822627]
50. Damen MSMA, Alarcon PC, Shah AS & Divanovic S Greasing the inflammatory pathogenesis of viral pneumonias in diabetes. Obes. Rev 23, e13415 (2022). [PubMed: 34989117]
51. Pujantell M & Altfeld M Consequences of sex differences in Type I IFN responses for the regulation of antiviral immunity. Front. Immunol 13:986840. [PubMed: 36189206]
52. Huang LY, Chiu CJ, Hsing CH & Hsu YH Interferon family cytokines in obesity and insulin sensitivity. Cells 11, 4041 (2022). [PubMed: 36552805]
53. Farr OM, Gavrieli A & Mantzoros CS Leptin applications in 2015: what have we learned about leptin and obesity? Curr. Opin. Endocrinol. Diabetes Obes 22, 353–359 (2015). [PubMed: 26313897]
54. Hellström L, Wahrenberg H, Hruska K, Reynisdottir S & Arner P Mechanisms behind gender differences in circulating leptin levels. J. Intern. Med 247, 457–462 (2000). [PubMed: 10792559]
55. Gilliver SC Sex steroids as inflammatory regulators. J. Steroid Biochem. Mol. Biol 120, 105–115 (2010). [PubMed: 20045727]
56. Mair KM, Gaw R & MacLean MR Obesity, estrogens and adipose tissue dysfunction - implications for pulmonary arterial hypertension. Pulm. Circ 10:2045894020952019.
57. O'Brien KB et al. Impaired wound healing predisposes obese mice to severe influenza virus infection. J. Infect. Dis 205, 252–261 (2012). [PubMed: 22147799]
58. Gay L et al. Sexual dimorphism and gender in infectious diseases. Front. Immunol 12:698121. [PubMed: 34367158]
59. Min J et al. Differential effects of sex on tuberculosis location and severity across the lifespan. Sci. Rep 13, 6023 (2023). [PubMed: 37055508]
60. Singh R et al. Association of obesity with COVID-19 severity and mortality: an updated systemic review, meta-analysis, and meta-regression. Front. Endocrinol. (Lausanne) 13:780872. [PubMed: 35721716]
61. Takahashi T et al. Sex differences in immune responses that underlie COVID-19 disease outcomes. Nature 588, 315–320 (2020). [PubMed: 32846427]
62. Szretter KJ, Balish AL & Katz JM Influenza: propagation, quantification, and storage Chapter 15, Unit 15G.1.1–15G.1.22. Curr. Protoc. Microbiol 2006.

Author Manuscript Author Manuscript Author Manuscript Author Manuscript

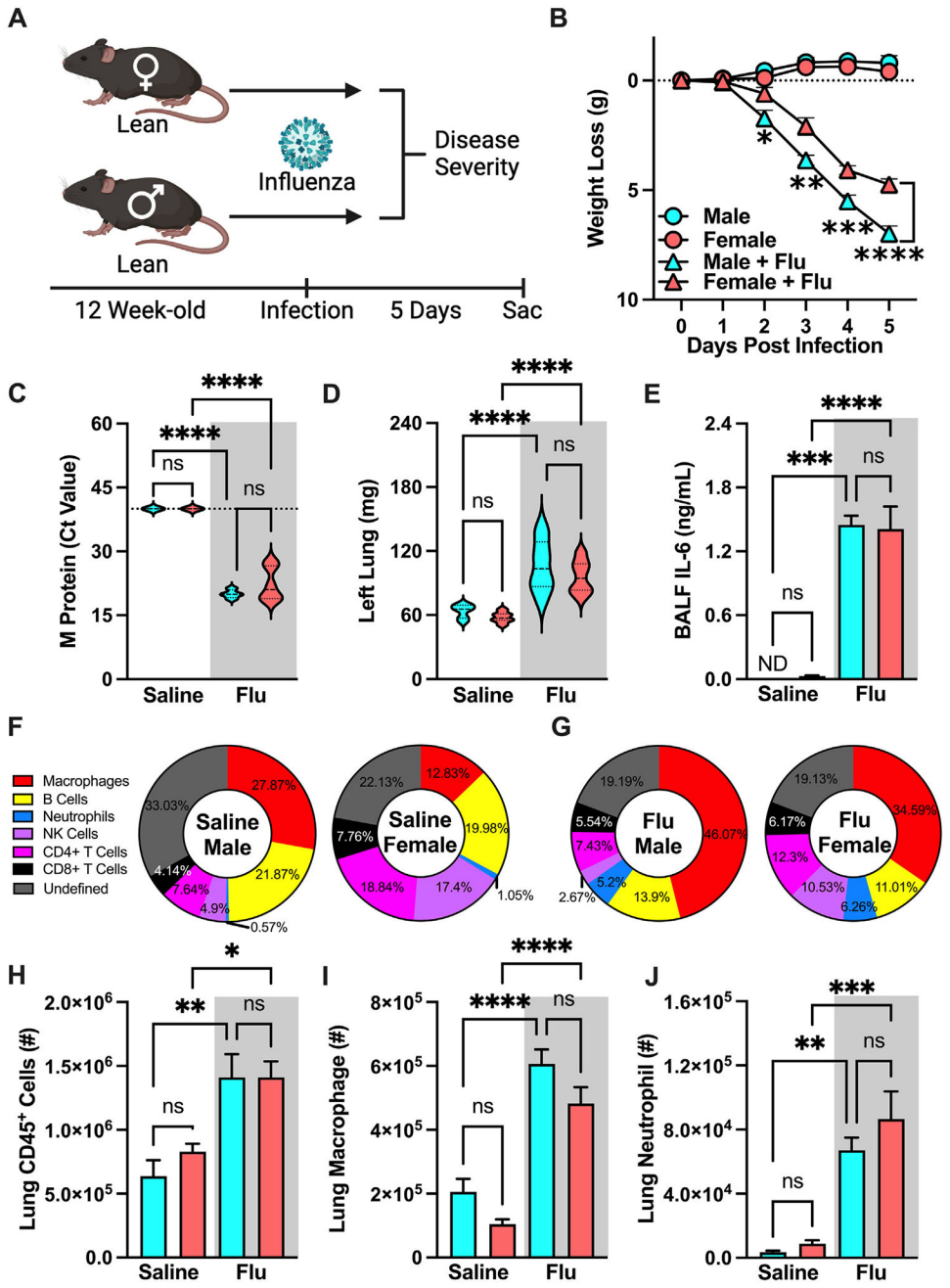

Fig. 1.

Lean female and male mice have similar influenza disease severity. (A) Experimental design schematic. 12-week-old WT C57/BL6 males and females (n = 6–13/group; combined result of 3 independent experiments) were intranasally mock-infected with saline or infected with influenza virus (Charles River Influenza A/PR/8/34 (H1N1), Batch: 4XP160913; dose of 30 Hemagglutinin (HA) units). (B) Weight loss post-infection. (C) Lung viral M protein expression quantified via qPCR. (D) Left lung weight 5 days post-infection. (E) Bronchoalveolar Lavage Fluid (BALF) Interleukin-6 (IL-6) levels quantified via cytokine ELISA. (F) Baseline immune cell population percentage of total lung $CD45^+$ cells.

Author Manuscript Author Manuscript Author Manuscript Author Manuscript

(G) Infected immune cell population percentage of total lung $CD45^+$ cells. (H) Lung $CD45^+$ immune cell infiltration, measured by flow cytometry as done previously by our lab[24,25]. (I) Lung macrophage absolute numbers ($CD11b^{hi}F4/80^{hi}$). (J) Lung Neutrophil absolute numbers ($CD11b^{hi}GR1^{hi}$). Means ± SEM. Student's t test or one-way analysis of variance; *$p < 0.05$, **$p < 0.01$, ***$p < 0.001$, ****$p < 0.0001$. ELISA = enzyme-linked immunosorbent assay; qPCR = quantitative polymerase chain reaction; SEM = standard error of the mean.

Author Manuscript Author Manuscript Author Manuscript Author Manuscript

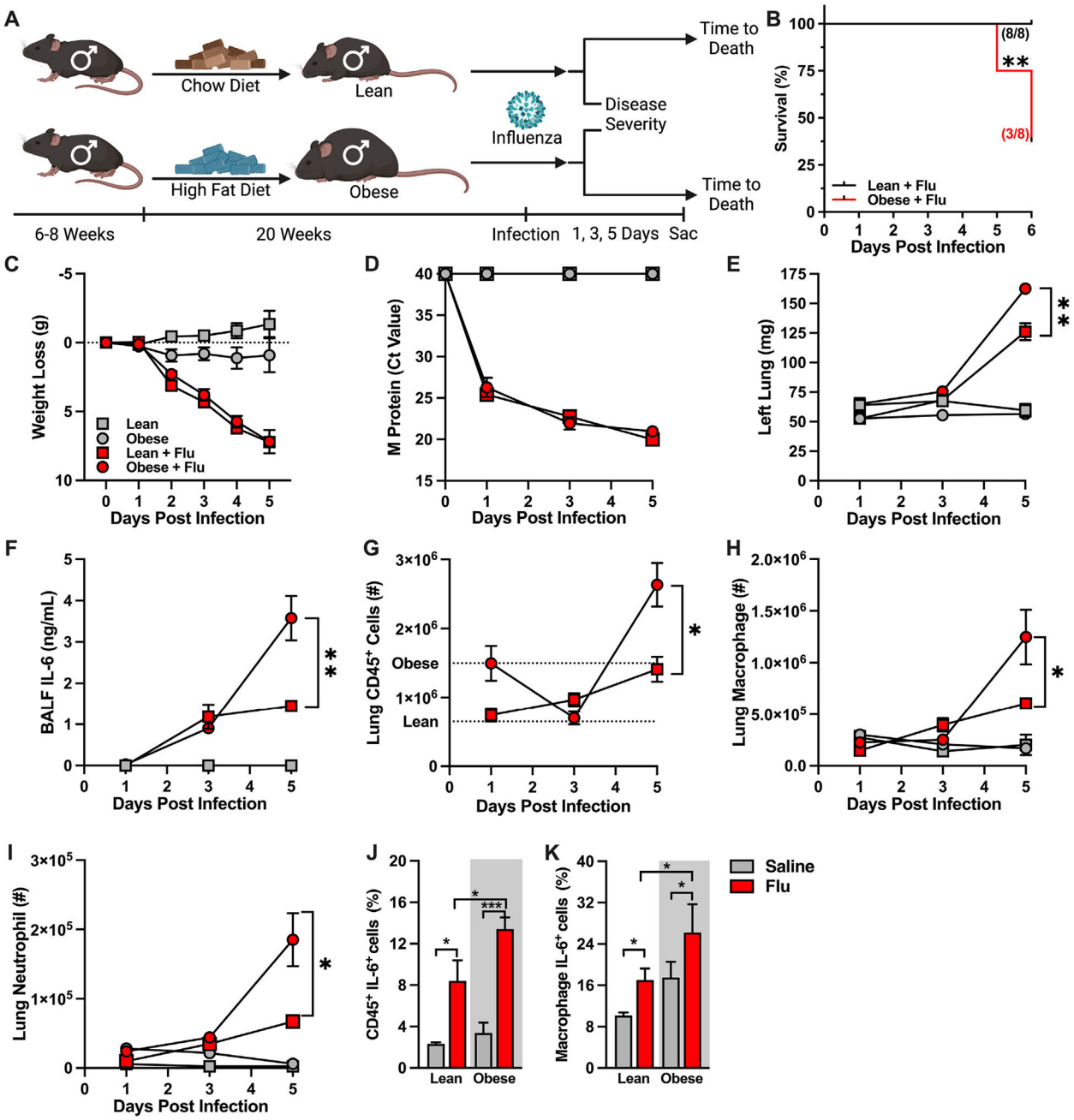

Fig. 2.

Obese male mice have increased lung inflammation in response to influenza infection compared to lean male mice. (A) Experimental design schematic. 6- to 8-week-old WT C57/BL6 males (3 independent experiments performed: 2 for time-to-death, 2 for kinetic analysis) were placed on either Chow Diet (CD, fat 10%, carbohydrate 70%, protein 20%; Research Diet #D12450J) or High-Fat Diet (HFD, fat 60%, carbohydrate 20%, protein 20%; Research Diet #D12492) for 20 weeks and subsequently intranasally challenged with saline or influenza virus. (B) Time-to-death curve of infected, lean, male and obese male mice (n = 8/group, result of 2 independent experiments). (C) Weight loss post-infection (n = 4–10/

Author Manuscript Author Manuscript Author Manuscript Author Manuscript

group; result of 2 independent experiments). (D) Lung viral M protein expression quantified via qPCR. (E) Left lung weight. (F) BALF IL-6 levels quantified via cytokine ELISA. (G) Total lung $CD45^+$ immune cell infiltration, measured by flow cytometry. Average of saline-treated controls represented by dashed lines. (H) Lung macrophage absolute numbers ($CD11b^{hi}F4/80^{hi}$). (I) Lung neutrophil absolute numbers ($CD11b^{hi}GR1^{hi}$). (J–K) Immune cell inflammatory capacity, performed via *ex vivo* PMA-Ionomycin and brefeldin stimulation. Inflammatory cytokine production quantified via intracellular antibody accrual via flow cytometry. (J) Total lung $CD45^+$ cell IL-6 production post *ex vivo* stimulation. (K) Lung macrophage IL-6 production post *ex vivo* stimulation. Means ± SEM. Student's t test or one-way analysis of variance; $*p < 0.05$, $**p < 0.01$. ELISA = enzyme-linked immunosorbent assay; PMA = phorbol 12-myristate 13-acetate; SEM = standard error of the mean; WT = wild-type.

Author Manuscript
Author Manuscript
Author Manuscript
Author Manuscript

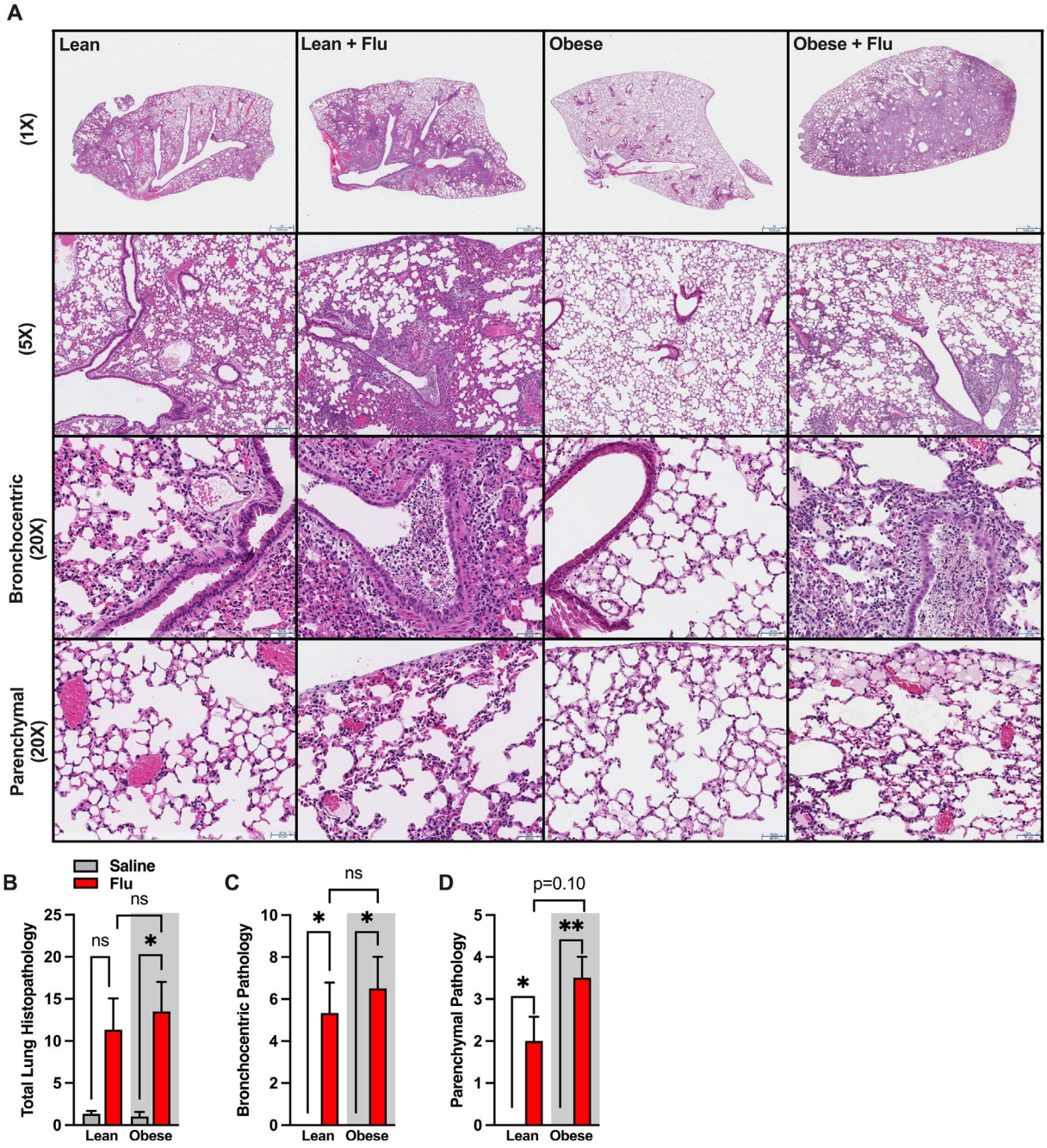

Fig. 3.

Infected obese male mice have worsened parenchymal inflammation than infected lean male mice. (A) Representative images of left lungs from lean and obese control/saline-treated versus influenza-infected mice (displayed in 4 columns), with no inflation, taken at different magnifications, equivalent to 1×, 5×, and 20× objectives (in rows; scale bars in micrometers; H&E stains). Low-power images provide overviews for each experimental group; intermediate power views zoom on main conductive airways (for bronchocentric pathology) and on peripheral alveolated lungs, to the pleura. Representative images for control (saline-infused during mock infection but not flushed or inflamed) lungs

Author Manuscript Author Manuscript Author Manuscript Author Manuscript

demonstrate both well-aerated air spaces and regions with minor procurement-related fresh hemorrhage. In control lean and obese mice, conductive airways are intact and free of bronchocentric pathologic processes (with no luminal, epithelial, transmural or peribronchial inflammatory infiltrates, or damage) and with no extension into the peripheral lung parenchyma—as reflected in histopathologic scores. For influenza-infected lungs, the bronchocentric distribution of increased cell density is apparent at low powers (1× and 5× equivalent), in contrast with the aerated peripheral parenchyma. At intermediate powers, the bronchocentric pathology ("20X", 3rd row) is evidenced by intraluminal purulent (necro)inflammatory infiltrates, attenuation of the inflamed broncho-epithelial lining, and extension to peribronchial spaces (with increased cellularity). Extension to the peripheral parenchyma ("20X" 4th row) is seen in dissipating small foci along alveolar septae, including in subpleural edema in occasional subjects (see obese infected mouse lung). (B) Total histopathological score for the entire lung. (C) Histopathological score of bronchocentric pneumonia (exemplified in images at "20X", 3rd row, and at low powers). (D) Histopathological score of inflammatory extension to parenchyma (exemplified at "20X", 4th row, and at low powers). H&E = hematoxylin & eosin.

Author Manuscript Author Manuscript Author Manuscript Author Manuscript

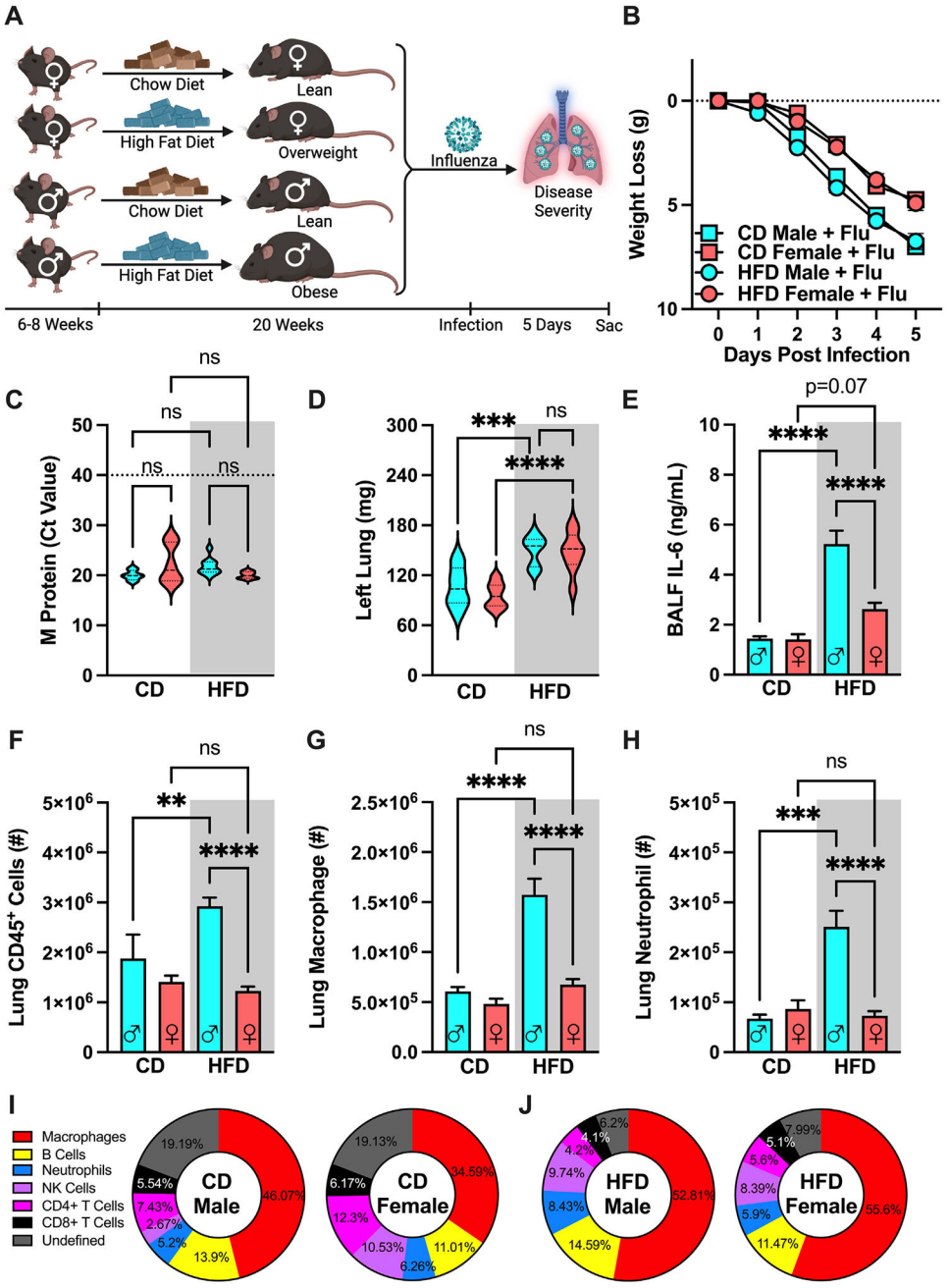

Fig. 4.

High-fat diet (HFD) feeding is not sufficient to robustly amplify influenza disease severity in female mice. (A) Experimental design schematic. 6- to 8-week-old WT C57/BL6 males and females (n = 8–14/group; combined result of 3 independent experiments) were placed on either CD or HFD for 20 weeks and subsequently challenged intranasally with influenza virus (30 HA Units). (B) Weight loss post-infection. (C) Lung viral M protein expression quantified via qPCR. (D) Left lung weight. (E) BALF IL-6 levels quantified via cytokine ELISA. (F) Total lung $CD45^+$ immune cell infiltration, measured by flow cytometry. (G) Lung macrophage absolute numbers ($CD11b^{hi}F4/80^{hi}$). (H) Lung neutrophil absolute

Author Manuscript Author Manuscript Author Manuscript Author Manuscript

numbers ($CD11b^{hi}GR1^{hi}$). Means ± SEM. (I) Infected immune cell population percentage of total lung $CD45^+$ cells in CD-fed males and females. (J) Infected immune cell population percentage of total lung $CD45^+$ cells in HFD-fed males and females. Student's t test or one-way analysis of variance; *$p < 0.05$, **$p < 0.01$, ***$p < 0.001$, ****$p < 0.0001$. CD = chow diet; ELISA = enzyme-linked immunosorbent assay; SEM = standard error of the mean; WT = wild-type.

Author Manuscript Author Manuscript Author Manuscript Author Manuscript

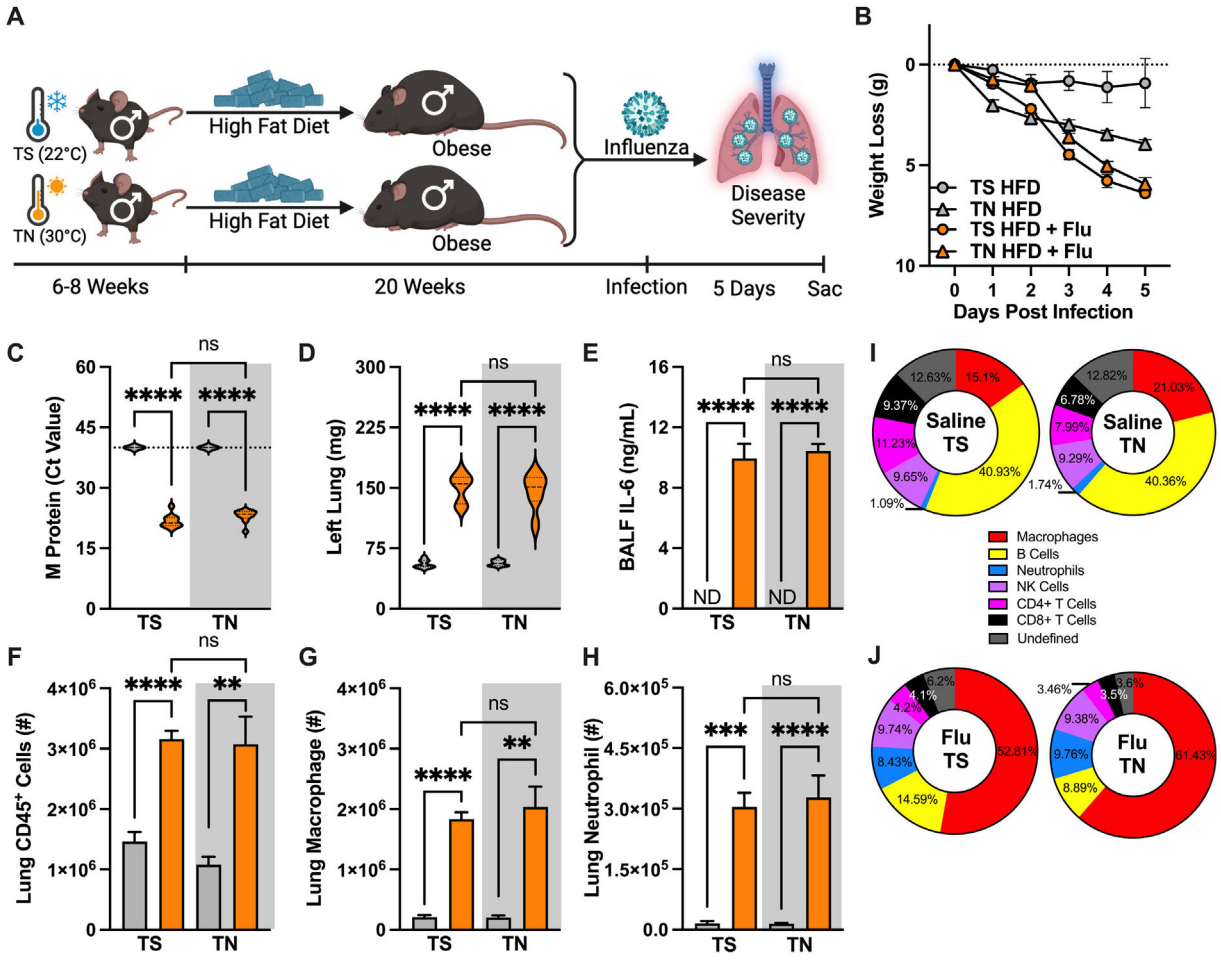

Fig. 5.

Obesity-associated influenza disease severity is maintained in thermoneutral (TN)-housed male mice. (A) Experimental design schematic. 6- to 8-week-old WT C57/BL6 males (n = 5–6/group; combined result of 2 independent experiments) were placed in either thermostress (TS, 22 °C) or TN (30 °C) housing and fed HFD for 20 weeks and subsequently challenged intranasally with influenza virus (30 HA units). (B) Weight loss post-infection. (C) Lung viral M protein expression quantified via qPCR. (D) Left lung weight. (E) BALF IL-6 levels quantified via cytokine ELISA. (F) Total lung $CD45^+$ immune cell infiltration, measured by flow cytometry. (G) Lung macrophage absolute numbers ($CD11b^{hi}F4/80^{hi}$). (H) Lung neutrophil absolute numbers ($CD11b^{hi}GR1^{hi}$). Means ± SEM. (I) Baseline immune cell population percentage of total lung $CD45^+$ cells in HFD-fed, TS- or TN-housed males. (J) Infected immune cell population percentage of total lung $CD45^+$ cells in HFD-fed, TS- or TN-housed males. Student's t test or one-way analysis of variance; $^{**}p < 0.01$, $^{***}p < 0.001$, $^{****}p < 0.0001$. BALF = bronchoalveolar lavage fluid; CD = chow diet; HFD = high-fat diet; IL-6 = interleukin-6; qPCR = quantitative polymerase chain reaction; SEM = standard error of the mean; WT = wild-type.

Author Manuscript Author Manuscript Author Manuscript Author Manuscript

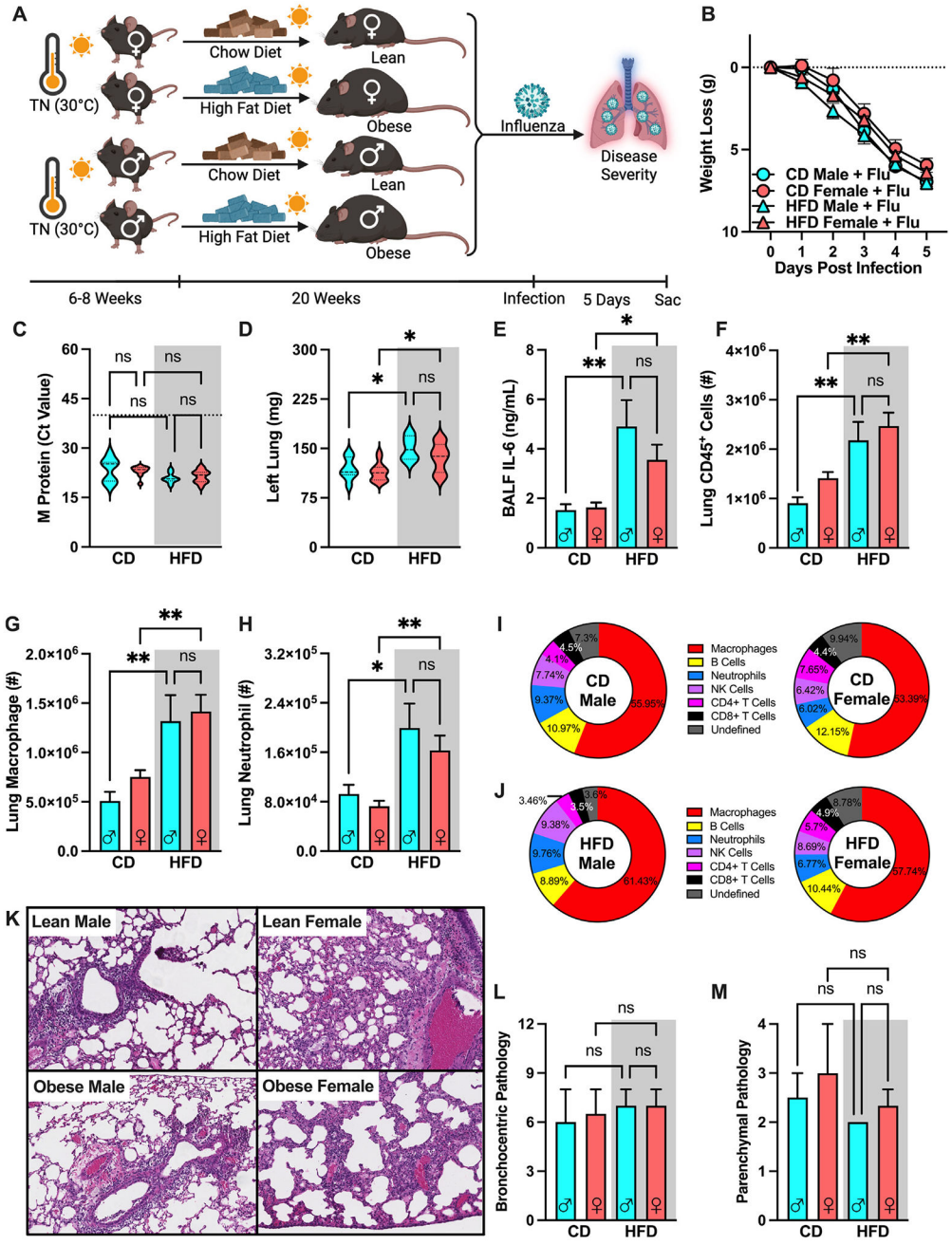

Fig. 6.

Obese male and female mice have comparably exacerbated obesity-associated influenza disease severity. (A) C57BL/6 male female mice (n = 6–15/group; combined results of 4 independent experiments) were placed in TN housing and fed CD or HFD for 20 weeks before intranasal challenge with influenza virus (30HA Units). (B) Weight loss post-infection. (C) Lung M protein expression quantified via qPCR. (D) Left lung weight 5 days post-infection (E) BALF IL-6 levels quantified via cytokine ELISA. (F) Total lung $CD45^{+}$ immune cell infiltration, measured by flow cytometry. (G) Lung macrophage absolute numbers ($CD11b^{hi}F4/80^{hi}$). (H) Lung Neutrophil absolute numbers ($CD11b^{hi}GR1^{hi}$). (I)

Author Manuscript Author Manuscript Author Manuscript Author Manuscript

Infected immune cell population percentage of total lung $CD45^+$ cells in TN-housed CD-fed males and females. (J) Infected immune cell population percentage of total lung $CD45^+$ cells in TN-housed HFD-fed males and females. (K) Histopathological score of bronchocentric pneumonia (L) Histopathological score of inflammatory extension to parenchyma. (M) Representative H&E staining of unflushed left lungs (light microscope, 10X). Means ± SEM. Student's t test or one-way analysis of variance; $^{**}p < 0.01$, $^{***}p < 0.001$, $^{****}p < 0.0001$. BALF = bronchoalveolar lavage fluid; CD = chow diet; ELISA = enzyme-linked immunosorbent assay; H&E = hematoxylin & eosin; HFD = high-fat diet; IL-6 = interleukin-6; SEM = standard error of the mean; TN = thermoneutral.

Author Manuscript Author Manuscript Author Manuscript Author Manuscript

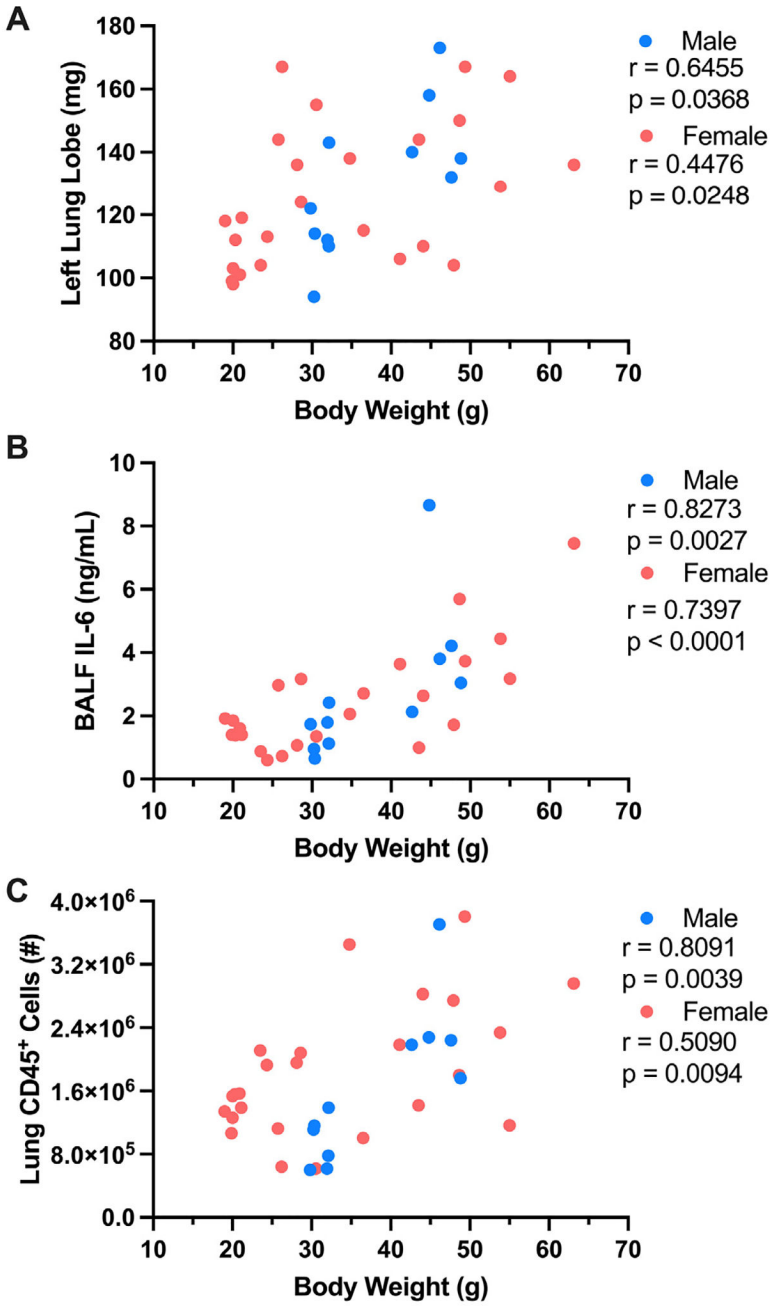

Fig. 7.

Increased total body weight correlates with worsened influenza-associated disease severity outcomes. Preinfection total body weight in TN-housed lean and obese males and females was correlated with various influenza disease severity metrics. (A) Preinfection total body weight versus left lung weight at 5 DPI. (B). Preinfection total body weight versus bronchoalveolar lavage fluid interleukin-6 levels at 5 DPI. (C) Preinfection total body weight versus Lung $CD45^+$ immune cell infiltration at 5 DPI. Nonparametric Spearman Rank Correlation and Pearson Correlation tests were performed for males and females,

Author Manuscript Author Manuscript Author Manuscript Author Manuscript

respectively, performed in Prism (GraphPad software). R *and p* values directly reported. DPI = days post-infection; TN = thermoneutral.

Author Manuscript Author Manuscript Author Manuscript Author Manuscript

Table 1.

Disease severity metrics for influenza-infected mice in thermostress housing.

Housing	**Thermostress**			
Diet	**CD**		**HFD**	
Sex	**Male**	**Female**	**Male**	**Female**
Weight loss (g)	6.983 ± 0.35	4.741 ± 0.26	6.750 ± 0.38	4.920 ± 0.34
Left lung weight (mg)	106.1 ± 8.55	95.93 ± 4.01	149.9 ± 5.85 *	147.9 ± 8.62 †
M protein (Ct Value)	20.00 ± 0.50	22.35 ± 1.01	21.74 ± 0.51	20.00 ± 0.36
BALF IL-6 (ng/mL)	1.450 ± 0.08	1.410 ± 0.21	5.231 ± 0.53 †	2.627 ± 0.25
Lung CD45^{+} cells (# × 10^{6})	1.876 ± 0.481	1.410 ± 0.126	2.924 ± 0.174 ‡	1.225 ± 0.0874
Lung macrophage (# × 10^{5})	6.063 ± 0.451	4.822 ± 0.514	15.74 ± 1.61 †	6.764 ± 0.535
Lung neutrophil (# × 10^{4})	6.713 ± 0.787	8.664 ± 1.71	25.12 ± 3.21 *	7.304 ± 0.925

All conditions reported as mean ± standard error of the mean (SEM). Ordinary one-way analysis of variance, statistical analysis compares HFD mice and their respective CD sex control (HFD male *vs.* CD male, HFD female *vs.* CD female).

= number; BALF = bronchoalveolar lavage fluid; CD = chow diet; HFD = high-fat diet; IL-6 = interleukin-6.

$^{\ddagger}p < 0.01$.

$^{\dagger}p < 0.0001$.

$^{*}p < 0.001$.

Author Manuscript Author Manuscript Author Manuscript Author Manuscript

Table 2.

Disease severity metrics for influenza-infected mice in thermoneutral housing.

Housing	**Thermoneutral**			
Diet	**CD**		**HFD**	
Sex	**Male**	**Female**	**Male**	**Female**
Weight loss (g)	6.956 ± 0.12	5.949 ± 0.42	7.050 ± 0.18	6.328 ± 0.28
Left lung weight (mg)	118.9 ± 6.34	114.3 ± 3.92	150.3 ± 9.40 *	136.3 ± 6.08 *
M protein (Ct Value)	23.36 ± 0.50	20.92 ± 0.54	23.03 ± 0.49	21.44 ± 0.54
BALF IL-6 (ng/mL)	1.526 ± 0.24	1.632 ± 0.20	4.905 ± 1.07 †	3.556 ± 0.61 *
Lung CD45^{+} cells (# × 10^{6})	0.9057 ± 0.118	1.412 ± 0.123	2.177 ± 0.373 †	2.469 ± 0.270 †
Lung macrophage (# × 10^{5})	5.087 ± 0.916	7.520 ± 0.680	13.18 ± 2.63 †	14.15 ± 1.69 †
Lung neutrophil (# × 10^{4})	9.250 ± 1.49	7.266 ± 0.890	19.93 ± 3.95 *	16.30 ± 2.41 †

All conditions reported as mean ± standard error of the mean (SEM). Ordinary one-way analysis of variance, statistical analysis compares HFD mice and their respective CD sex control (HFD male *vs.* CD male, HFD female *vs.* CD female).

= number; BALF = bronchoalveolar lavage fluid; CD = chow diet; HFD = high-fat diet; IL-6 = interleukin-6.

$^{*}p < 0.05$.

$^{\dagger}p < 0.01$.